BOLETIN DE LA SOCIEDAD ESPAÑOLA DE
Cerámica y Vidrio
www.elsevier.es/bsecv

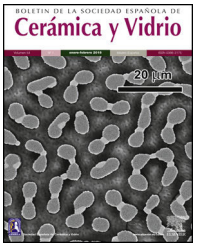

Effect of the drying procedure on hybrid sono-aereogels for organic solvent remediation

María Reyes-Peces[a,*], *Beatriz Amaya-Dolores*[a], *Víctor Morales-Flórez*[b], *Desirée de-los-Santos*[c], *María del Mar Mesa*[d], *Luis Esquivias*[b], *Nicolás de-la-Rosa-Fox*[a], *Manuel Piñero*[a]

[a] *Departamento de Física de la Materia Condensada, Universidad de Cádiz, Puerto Real (Cádiz), Spain*
[b] *Departamento de Física de la Materia Condensada, Universidad de Sevilla, Sevilla, Spain*
[c] *Departamento de Química Física, Universidad de Cádiz, Puerto Real (Cádiz), Spain*
[d] *Departamento de Ingeniería Química, Universidad de Cádiz, Puerto Real (Cádiz), Spain*

ARTICLE INFO

Article history:
Received 12 November 2022
Accepted 2 March 2023
Available online 21 March 2023

Keywords:
Sono-aerogel
DEDMS-TEOS
Supercritical CO_2
Superhydrophobic
Ambigel
Organic solvent remediation

ABSTRACT

Hybrid organic–inorganic aerogels are highly hydrophobic porous solids that avoid the brittleness and moisture adsorption of the standard silica aerogels. Superhydrophobic porous materials have attracted great interest because of their ability for selective absorption of organic solvents while repelling water, as excellent candidates for remediation techniques. This work shows a comparative of three drying procedures of DEDMS/TEOS (diethoxydimethylsilane/tetraethylorthosilicate) gels, namely, by supercritical CO_2, by supercritical ethanol, and dried at ambient conditions. Supercritical CO_2 and ambient drying produced superhydrophobic aerogels ($\theta > 150^{\circ}$), while supercritical ethanol drying produces denser aerogels with smaller both porous volume and specific surface area. Regarding the absorption of organic liquids, swelling is observed in all cases. Hexane had faster diffusion that obeyed Fick's law ($\propto t^{0.5}$) whereas liquid polydimethylsiloxane exhibited slower non-Fickian diffusion process ($\propto t^{n}$, $n < 0.5$).

Influencia del procedimiento de secado en sono-aerogeles híbridos para la eliminación de solventes orgánicos

Palabras clave:
Sono-aerogel
DEDMS-TEOS
CO_2 supercrítico

RESUMEN

Los aerogeles híbridos orgánicos-inorgánicos son sólidos porosos altamente hidrofóbicos, que mejoran la fragilidad e impiden la absorción de humedad típicas de los aerogeles de sílice. El estudio de materiales superhidrofóbicos porosos ha generado gran interés debido a la capacidad que estos poseen para absorber de forma selectiva solventes orgánicos, mientras repelen el agua, resultando ser excelentes candidatos en técnicas de remediación

* *Corresponding author.*
E-mail address: maria.reyes@uca.es (M. Reyes-Peces).
https://doi.org/10.1016/j.bsecv.2023.03.001

Superhidrofóbico
Ambigel
Eliminación de solventes orgánicos

ambiental. En el presente trabajo se comparan tres métodos de secado de geles de dietoxidimetilsilano/tetraetilortosilicato (DEDMS/TEOS), concretamente realizados en atmósfera supercrítica de CO_2, en etanol supercrítico y, por último, en condiciones ambientales. Mientras los procedimientos de secado llevados a cabo en CO_2 supercrítico y en condiciones ambientales producen aerogeles superhidrofóbicos ($\theta > 150^\circ$), el realizado en etanol supercrítico dio lugar a aerogeles de mayor densidad, con menor volumen poroso y superficie específica. En cuanto a la absorción de líquidos orgánicos, en todos los casos tiene lugar el hinchamiento de la red polimérica (*swelling*). El hexano presentó una difusión rápida, que obedece a la ley de Fick ($\propto t^{0,5}$), mientras que el polidimetilsiloxano líquido mostró un proceso de difusión más lento que no obedece la ley de Fick ($\propto t^n$, $n < 0,5$).

Introduction

Industrialization and urbanization in developed and emerging nations have had significant negative consequences for freshwater and seawater ecosystems. Industrial wastewater is one of the most important sources of contamination, which includes very diverse organic compounds and suspended solids that must be removed or reduced to limit pollution by basic or complex wastewater treatment facilities. Water-soluble organic compounds usually degrade faster than lipophilic compounds, which are particularly most persistent, resulting in the accumulation of specific industrial contaminants, many of them with associated toxic effects. Hence, one of the most urgent tasks for environmental preservation is to reduce the huge accumulation of water contaminants. To address this challenge, several remediation techniques have been developed and a large number of experiments to evaluate their efficiency have been reported [1,2]. One of the most important remedies for oil or organic solvents spills in practice is mechanical recovery by the use of sorbent materials. Among these, superhydrophobic absorbers show noteworthy benefits such as selectivity to absorb oil or organic solvents. Various examples that have been studied involve modified organophilic clays, silica, exfoliated graphite, polyurethane sponges, cellulose-based materials and polydimethylsiloxane elastomers and hybrid gels [3]. Also, materials derived from silica aerogels materials have been used for oil sorption [4–6]. This type of material is very attractive due to its high specific surface area, pore volume and low density, together with a high mechanical stability, which makes them inspiring proposals for remediation techniques.

Silica aerogels are complex structures which consist of a coherent solid 3D-network formed by the bonding and arrangement of nanometric-sized silica particles (3–4 nm in diameter), to give hierarchically-ordered structures or randomly-arranged particles [7]. They are extremely porous (pore volume higher than 85%) with an average pore size between 30 and 50 nm, and they have very low density (<5 kg/m^3) and large surface area (>500 m^2/g). Nevertheless, the potential applications of aerogels always appear limited by their poor mechanical properties. For example, under compression, they exhibit classical fragile fracture, after undergoing small plastic deformation due to pore collapse, which is favoured by the large pore structure and loose cluster structure [8].

Also, the extreme fragility response under stress due to high absorption of water make it difficult to maintain its physical integrity when being handled [9]. The inclusion of polymers based on Si–C bonds, such as polydimethylsiloxane (PDMS), are a solution to avoid problems derived from fragility and/or moisture absorption, as it modifies the inorganic network of the silica aerogels and creates homogenous organic–inorganic hybrid materials with physical and mechanical properties that can be modulated depending on the composition [10–12].

These type of aerogels are typically obtained by, firstly, processing of alcogel by the sol–gel method. This step can also be assisted by the use of ultrasound (sonocatalysis), which significantly affects the chemical reactions and gelation rate, improving the thermal stability and increasing the apparent density of the resulting sonogels [13,14] and secondly, removing pore residual solvent from wet gel in an autoclave, at temperatures and pressures slightly higher than the critical point of a predetermined fluid (typically CO_2 or ethanol). The SiO_2-PDMS sono-aerogel was first obtained by Kramer et al. [10], by removing the pore solvent under supercritical CO_2 conditions. Due to its easily accessible critical conditions (31 °C, 7.39 MPa), CO_2 is the most widely used supercritical fluid to obtain this type of material. Hence, it enables carrying out the process at mild temperatures (40–60 °C). This procedure makes it possible for the microstructure of the wet hybrid sonogel in a dry form to be preserved as a monolithic sample. Following this drying method, the synthesis of a lot of new silica-based hybrid aerogels combining different organic compounds has been proposed [15]. Alternatively, hybrid SiO_2-PDMS monolithic sono-aerogels with a high content in the organic phase were successfully obtained using supercritical ethanol (241 °C, 6.1 MPa). Thermal analysis demonstrated that the organic chains in these samples do not degrade thermally until 260 °C under inert atmosphere [16].

In the case of conventional drying, a xerogel is obtained, in which, commonly, the very high porous structure has collapsed, yielding denser hybrid samples. Other procedures use chemical additives that reduce the surface tension of the liquid–vapor interphase, reducing the capillary pressure during drying, and avoiding pore collapse during conventional

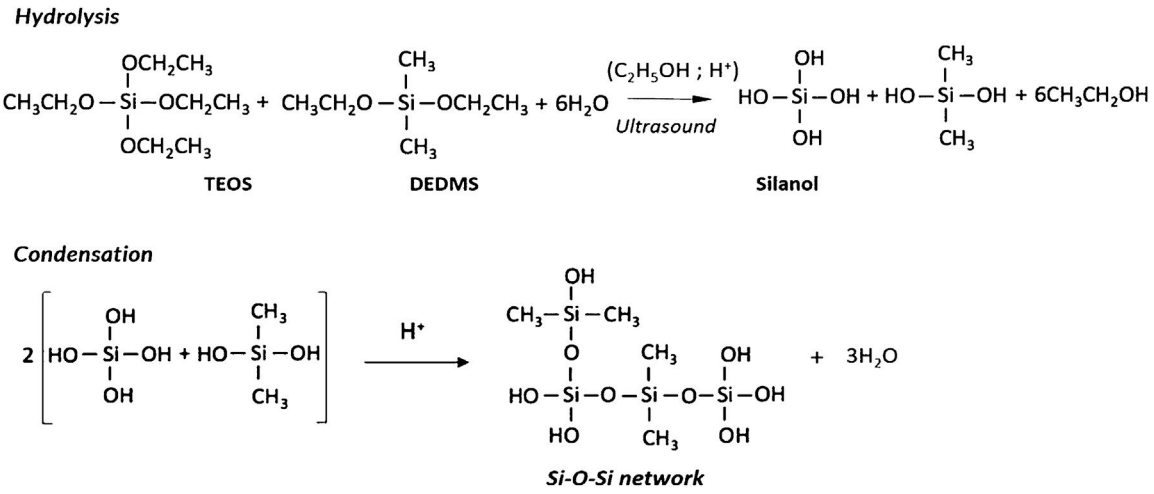

Scheme 1 – Hydrolysis and condensation reactions between TEOS and DEDMS in acidic media.

drying. Samples obtained through this method are known as ambigels.

These different drying processes have been researched and discussed previously. For example, the higher temperatures used during ethanol-dried supercritical drying process, in comparison to the CO_2-based process, yield hydrophobic silica aerogels, while CO_2-dried silica aerogels are hydrophilic [17,18].

These hybrid aerogels acquired an elastomeric type of behaviour, instead of the characteristic brittle behaviour of the pure silica aerogels, and the resulting porosity and specific surface area decreased to a great extent due to the addition of the organic phase. Beyond this simple modification in the microstructure and the mechanical properties, hybrid aerogels are also hydrophobic and superhydrophobic nanostructures [7,9,19]. In other words, these procedures allow the fabrication of highly homogeneous hybrid materials with tuneable physicochemical properties, with a wide range of compositions [20]. For example, in a previous work [5], monolithic sono-aerogels using tetraethoxysilane (TEOS) and diethoxydimethylsilane (DEDMS) as the organic component were successfully obtained by performing supercritical drying in ethanol. The results showed how increasing the organic content produced a significant decrease in the specific porous volume, from 3.31 to 0.14 cm^3/g, and the specific surface, from 900 to 40 m^2/g, for pure silica aerogel and the rubbery TEOS-DEDMS 50 wt.% aerogel (1:1.25 molar ratio), respectively. Otherwise, the presence of the methyl radicals made the silica aerogels superhydrophobic and oleophilic. Thus, due to these new properties, the TEOS-DEDMS sono-aerogels were successfully used to selectively separate silicone and hydrocarbon oils from water, exhibiting a high absorption capacity, fast absorption and excellent reusability.

The first objective of the present study was to study the effects of the different drying conditions on the structural, physicochemical and mechanical properties, of different sets of hybrid silica-organic samples: aerogels dried through supercritical ethanol, through supercritical CO_2, and one conventionally ambient-dried sample, that is, a xerogel. Secondly, the absorption performance of these hydrophobic TEOS-DEDMS samples has been tested for different solvents. Lastly, the mechanical properties of both the as-prepared (dry) samples and those immersed in PDMS organic solvent (wet) states have also been compared in order to discuss the reusability of the samples for their technological applications as wastewater cleaners.

Materials and methods

Synthesis of hybrid samples

The synthesis of the hydrophobic samples in this study involved two major steps: the preparation of the alcogels and the drying procedure. The chemical reactions responsible for the formation of three-dimensional gel network are outlined in Scheme 1.

Initially, tetraethoxysilane (TEOS) was mixed with diethoxydimethylsilane (DEDMS) in absolute ethanol (EtOH) solvent and were totally hydrolyzed with water under acidic conditions with nitric acid (0.1 M). The DEDMS/TEOS molar ratio was fixed to 1.25, corresponding to 50 wt.% of the organic phase with regard to the total silica content of the sample. The first step is the condensation of these hydrolyzed species by a one-step acid-catalyzed sol–gel process in ethanol solvent to get the alcogels, followed by their ageing soaked in ethanol for four weeks at 50 °C and then being washed in new ethanol for three days at ambient temperature before being subjected to drying. All chemical reactions were carried out under the catalytic effects of ultrasound, by supplying 0.6 kJ/cm^3 of high power ultrasound, in a flask immersed in a cooling bath at 0 °C.

The drying procedures

The second step for the synthesis of the samples is the drying of the gels to remove the solvent. This second step was performed by three different procedures: in supercritical ethanol, in supercritical carbon dioxide, and by ambient evaporation at atmospheric pressure. By means of these procedures, cylindrical monolithic samples were obtained, with heights

Table 1 – Sample code and drying conditions.

Sample	Atmosphere	T (°C)	P (MPa)
TD0	Ethanol	270	8
ScEt	Ethanol	270	8
$ScCO_2$	CO_2	40	10
AD	Air	25	0.1

of 15–20 mm and diameters of 8–10 mm. The samples were labelled as "ScEt", "$ScCO_2$" and "AD", for drying performed under supercritical ethanol, supercritical CO_2 and ambient drying conditions, respectively. In addition, pure silica aerogels were also synthesized from TEOS by sol–gel, followed by supercritical drying in ethanol, (referred to as "TD0") as a reference, in order to make pertinent comparisons with the hybrid aerogel samples. All the samples were kept at 50 °C in an oven for stability. In summary, 45 TEOS-DEDMS samples were prepared, 15 for each drying procedure, plus 5 pure silica aerogels. The critical temperatures and pressures of the solvents, conditions of their synthesis (temperature and pressure), and the designations of the samples are summarized in Table 1.

Characterization of the samples

The density of the samples was obtained by measuring the mass and the volume of the cylindrical samples with a microbalance (precision ± 0.1 mg) and a calliper (precision ± 1/20 mm), respectively. The nanostructural characteristics of the hybrid aerogels (texture) were investigated by means of nitrogen physisorption experiments (Micromeritics ASAP2010, working at 77 K and equipped with pressure transducer resolution of 10^{-4} mmHg). The specific surface area, specific pore volume and pore diameter were determined, using standard models for the analysis (BET and BJH, respectively). Prior to these experiments, the samples were milled in an agate mortar and degasified at 150 °C for 2 h at 100 Pa. Thermogravimetric analysis (TGA) was performed with a TGA Q50, TA Instruments, thermogravimetric analyzer at a heating ramp of 10 °C/min under N_2 atmosphere. The initial degradation temperature and the residual weight were determined. The microstructural surface morphology was studied by scanning electron microscopy (SEM) with a thermoionic filament emission (FEI Quanta; resolution: 3.5 nm) using the low-vacuum capability in the pressure range 10–130 Pa, which enables the analysis of wet specimens without previous preparation. The hydrophobicity of the samples was studied by measuring the contact angle θ using the sessile drop method: a drop of 5 μL is deposited on the flat surface of the aerogel with a micro syringe of 50 μL DS 500/GT. The values of the static contact angle were determined using a commercial video-based software-controlled contact angle analyzer (SCA22, model OCA 15plus, from Dataphysics Instruments). The chemical structure was studied by Fourier transform infrared spectroscopy (FTIR). All the infrared spectra were collected at room temperature by a Fourier transform spectrometer (Bruker Tensor 37) with a resolution of 4 cm^{-1} and 32 scans in the region 4000–400 cm^{-1}. The samples were stored overnight in a stove at 60 °C, then ground and mixed with KBr and pressed into a self-supporting wafer. The wafer was put on a sample holder for the spectrum collection.

Liquid absorption

For the liquid absorption experiments, the cylindrical specimens of the hybrid samples were immersed in two different organic solvents up to the point of saturation at room temperature (20 ± 2 °C). A silicone oil (silanol-terminated PDMS) fluid of medium viscosity (450 g/mol in average molar mass, density = 0.965 g/cm^3, viscosity = 20–32 cSt at 15 °C) was used as the reference oily fluid; and n-hexane (density = 0.692 g/cm^3) as a reference for hydrocarbon liquid. The samples were removed periodically from the liquid bath to measure their weight in a sensitive microbalance. Before each measurement was made, the excess surface liquid was wiped off of the specimen. After the weight was registered, the sample was immediately returned to the liquid bath. This process was repeated until no weight change was observed for several hours, at which time the saturation of the absorption test is attained. The liquid absorption process was studied by measuring the relative weight gain $M(t)$ defined in terms of the mass of the absorbed fluid per mass of the dry sample, that is, the actual mass for a given time, $m(t)$, minus the mass of the dry sample, $m(0)$, divided by the mass of the dry sample (Eq. (1)):

$$M(t) = \frac{m(t) - m(0)}{m(0)} \quad (1)$$

The time-dependence of the normalized weight gain, $M(t)/M_\infty$, was registered for the kinetic studies, where M_∞ is the weight of the sample after saturation (namely, for $t \to \infty$). Finally, the absorption capacity was also assessed as the ratio of the volume of absorbed liquid compared to the original porous volume of the sample, revealing the presence of swelling if this ratio exceeds unity.

Mechanical tests

The mechanical tests were performed by uniaxial compression on the as-prepared samples (dry), and also on the samples immersed in liquid silicone oil after saturation in the absorption experiments. Uniaxial compression tests were performed in a Shimadzu universal testing machine, AG-I Autograph, equipped with a load cell of 5 kN (within ±1% of the indicated test force at a load cell rating of 1/250). For the dry samples, a sample deformation rate of 0.5 mm/min was considered; for the wet samples, this rate was 0.01 mm/min. Compression was performed until the breakage of the sample was achieved. The mechanical parameters were obtained by unconfined compression from cylindrical specimens of 15–20 mm in height and 8–10 mm in diameter, in accordance with the ASTM D7012 standard. The compressive strength was obtained from the maximum stress before sample failure, and the elastic modulus was estimated from the slope of the stress–strain curve. All the dry experiments were performed in triplicate to get statistical significance. The wet experiments were performed once.

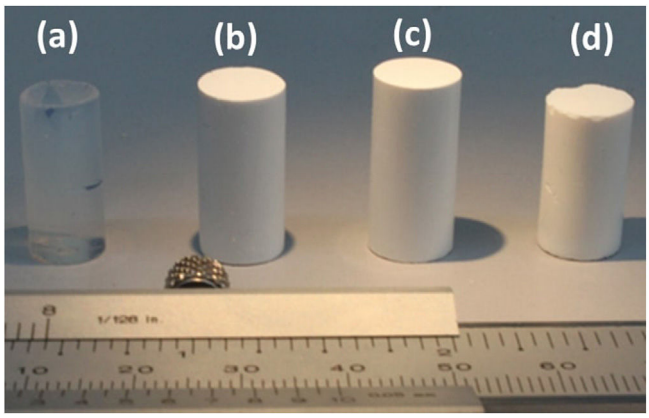

Fig. 1 – Examples of the samples studied in this work: (a) TD0; (b) ScEt; (c) $ScCO_2$; (d) AD.

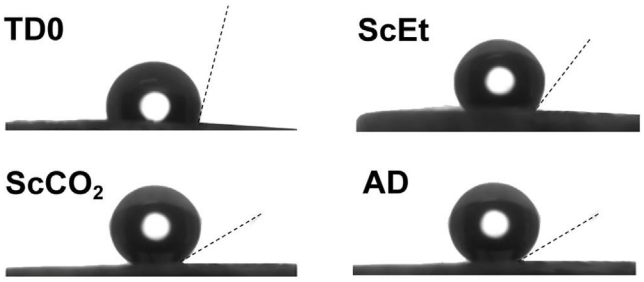

Fig. 2 – Water contact angles on TD0 and hybrid samples.

Results and discussion

Density, contact angle, microstructure and chemical properties

The TEOS-DEDMS samples were obtained as monolithic cylinders (Fig. 1). Sample TD0 was a typical silica aerogel, produced through an acid-catalyzed sol–gel process, transparent and brittle, with a density of $\rho = 0.32 \pm 0.04\ g/cm^3$. In contrast, hybrid specimens were opaque, with average bulk densities ranging from $\rho = 0.38$ to $0.41\ g/cm^3$ (see Table 2). Although these densities seem higher than those observed in the literature for classical aerogels [s10853.-014-8480-0], they are typical values obtained when ultrasound is used in the sol–gel process [5,21].

Contact angle

The measurement of the hydrophobicity of the samples revealed that the copolymerization with DEDMS made the samples hydrophobic, as can be clearly seen in Fig. 2, in which the composition and the influence of the drying procedure are compared. The obtained values of the contact angles are listed in Table 2. Samples dried in ethanol were both hydrophobic, with contact angles $\theta = 91^\circ \pm 2^\circ$ and $\theta = 128^\circ \pm 2^\circ$, for samples TD0 and ScEt, respectively. The surfaces of the $ScCO_2$ and AD samples showed a contact angle of $\theta > 150^\circ$, similar to confirming their superhydrophobicity. These results are in agreement with those of previous studies of polysiloxane aerogels obtained in a similar manner [22,23].

This hydrophobic surface behaviour is the combined result of the copolymerized DEDMS/TEOS, which contributes hydrophobic methyl radicals, and the surface roughness of the mesoporous aerogels [24]. Therefore, the addition of the organic chains of DEDMS confers significantly higher hydrophobicity to the nanoporous silica structure. Surprisingly, despite the high temperatures employed in the ethanol-based drying procedure, which involves the hydrophobization of the silica [25], superhydrophobic samples were only obtained by the CO_2-based and ambient drying procedures. In previous work, contact angles very close to 0° for common motor oil in TD0 and ScEt samples were obtained, thus confirming the good oleophilicity and, in addition, the expected ability of these samples for oil recovery from wastewaters [5].

Nitrogen physisorption

The characteristic microstructural features of these samples were revealed by physisorption experiments. The corresponding adsorption/desorption isotherms are shown in Fig. 3. The TD0 isotherm is type IV, based on the IUPAC classification, and is associated with capillary condensation through multilayer adsorption taking place in interconnected mesopores, leading to a type H1 hysteresis loop. The TD0 sample presented typical high specific surface area ($921\ m^2/g$) and pore volume ($1.99\ cm^3/g$), with mean pore size 9.2 nm and a monomodal pore size distribution, as expected for ethanol-dried pure silica aerogel, as shown in Table 2.

The other adsorption curves, for the hybrid samples (Fig. 3), can be classified as type II, which behave like porous media containing both macropores and mesopores. Unclosed hysteresis loops belong to type H3, which is often attributed to

Table 2 – Bulk density, averaged water contact angle, specific surface area, specific pore volume and mean pore size obtained from N_2 physisorption, for pure silica TD0 aerogel, and hybrid aerogels. Specific surface area S_{BET} correlation coefficient in BET fitting was higher than 0.999 in all cases. Characteristic pore sizes are estimated from the position of the peak of the pore size distribution.

Sample	Density, ρ ($\pm 0.04\ g/cm^3$)	Contact angle, θ (°)	S_{BET} (m^2/g)	V_p (cm^3/g)	Pore size (nm)
TD0	0.32	91 ± 2	921	1.99	9.2
ScEt	0.41	128 ± 2	80	0.23	41.3
$ScCO_2$	0.38	153 ± 1	265	0.36	55.3
AD	0.38	151 ± 5	257	0.42	54.0

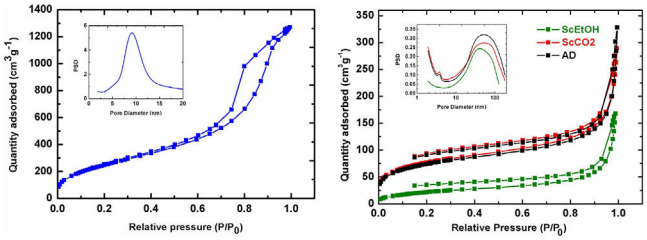

Fig. 3 – Nitrogen adsorption isotherms and pore size distributions (insets) for pure silica sonoaerogel TD0 sample (left), and for hybrid samples (right). Note the different scale of the vertical axis.

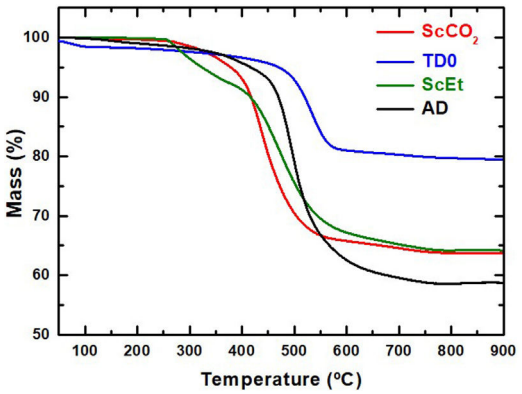

Fig. 4 – TG curves from TD0 and hybrid samples.

narrow slit-shaped micropores in which the release of trapped nitrogen is difficult owing to a slow diffusion rate, which hinders reaching the equilibrium during desorption and prevents the closure of the hysteresis loop. This phenomenon may be intensified by the presence of ink-bottle pores [26] and perseveres, despite increasing the data sampling of the isotherms or doubling the equilibrium time during desorption. These qualitative structural changes can be explained in terms of the composition of the sample, given that the hybrid aerogels are made with a 1:1.25 DEDMS:SiO_2 molar ratio (50 wt.% organic:inorganic mass ratio) so the percolation level of the organic phase (40 wt.%) was already exceeded [12]. For these reasons, the hybrid aerogels studied in this work can be considered as an organic matrix where the silica clusters are embedded, instead of a porous silica matrix with embedded polydimethylsiloxane oligomers.

The presence of DEDMS in the hybrid samples drastically decreases the specific surface area to above 260 m^2/g in the case of the $scCO_2$ and AD samples, and to 80 m^2/g for the scEt aerogel. This decrease is similar to what has been reported previously [5] and the differences from the AD are also expected due to the collapse of the structure and densification. However, the different supercritical drying procedures produced significant differences in the submicrostructure of the aerogels. Thus, completely similar alcogels resulted in aerogels with more open structures when dried with supercritical CO_2 instead of ethanol, with lower density, higher specific surface area and pore volume, and a finer pore size. In addition, the pore size distributions of all the hybrid samples showed similar characteristic pore sizes in the range of 41.3–54.0 nm (Table 2), that is in the limit between the meso- and macropore domains. This fact is corroborated by the closed hysteresis loop for the TD0 sample without micropores, compared to the open loops for the other samples.

Thermal stability

The initial degradation atmosphere and thermal stability was studied by thermogravimetric analyses under inert atmosphere (Fig. 4). The weight loss of silica aerogel (TD0) initiates below 250 °C with the extraction of adsorbed water and increases continuously up to 700 °C. The total weight loss corresponds to a higher condensation of surface silanol groups (dehydroxilation) than expected for fully dense silica particles with 921 m^2/g and exhibiting the typical surface OH density of ~4–5 OH per nm^2 [17]. Thus, some loss of organic components (such as ethanol or ethoxy groups) and of structural water can be concluded. Moreover, it can also be confirmed that the thermal degradability is greatly affected by the choice of the drying method. For example, the decomposition of the aerogel ScEt started at a lower temperature than that of the samples $ScCO_2$ and AD, and was similar to TD0. It exhibited two differentiated processes: the first one is due to the condensation of silanols of the surface and the degradation of the ethoxy radicals originating during the ethanol-based drying process [27], and the second one due to the degradation of the organic phase, mainly attributed to the decomposition of methyl groups [28].

The samples TD0, AD and $ScCO_2$ showed a one-step degradation process and more stable organic phases (degradation at higher temperatures). These results revealed that the thermal stability of the organic phase in this type of sample can be better achieved through mild drying temperatures, between 40 and 50 °C, instead of the 270 °C used in the case of the ScEt sample. The total weight loss of the AD sample is higher than those of the ScEt and $scCO_2$ samples. Assuming the full degradation of the organic phase (the same in all hybrid samples), this is due to the lower temperature of the drying process when working in ambient drying than with supercritical ethanol, which leads to a higher hydroxyl surface density.

FTIR

The typical FTIR spectra obtained for the samples are shown in Fig. 5. The observed absorption bands agree with a predominant inorganic silica network composed of Si–O–Si bonds, with two methyl groups per silicon and hydroxyl groups at the network ends [29]. Thus, three bands centred at 800, 1040, and 1100 cm^{-1} associated with the Si–O–Si asymmetric and symmetric stretching vibration modes are found in the four samples [30]. Absorption bands corresponding to stretching vibrations of Si–C bonds at 850 cm^{-1} and symmetric and asymmetric flexural vibrations of $Si–CH_3$ group at 1265 and C–H bending at 1400 cm^{-1} confirm the existence of methyl groups in the hybrid structures [31,32]. Also, symmetric and asymmetric stretching vibrations of C–H bonds between 2800 and 3000 cm^{-1} accounts for residual ethoxy radicals in TD0 and ScEt [33] in coherence with the degradation processes observed in TGA (Fig. 3). This band is clearer in the $ScCO_2$

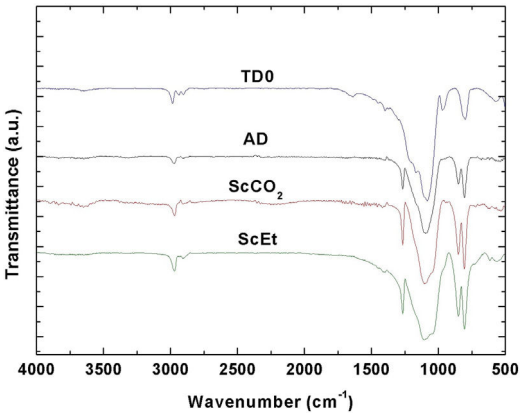

Fig. 5 – FTIR spectra obtained in the samples TD0 and hybrid samples.

sample and demonstrates the great extent of the condensation reactions favoured by its drying procedure. Two additional bands accounting for surface Si–OH and H–O–H bonds are found at 961 and 1640 cm^{-1} respectively, in the TD0 sample [31]. Also narrow peaks at 1100 and 1200 cm^{-1} probably indicate that the TEOS molecule is not fully hydrolyzed. Therefore, the band at 961 cm^{-1} in TD0 could also account for ethoxy non-hydrolyzed groups. Finally, it is worth noting the almost complete absence of any absorption peak in the region of 3500 cm^{-1}, associated with O–H vibrations, therefore indicating the deficiency of hydroxyl groups on the surfaces of the aerogels and the strong hydrophobic character of all the samples [28].

Scanning electron microscopy

A comparison of the scanning electron micrographs of the samples was also performed. Fig. 6a shows the regular surface aspect of the inorganic silica aerogel TD0, with extremely fine structural features, far below the 500 nm length scale. In contrast, some differences are clearly seen with Fig. 6b, c and d, from ScEt, $scCO_2$, and AD, respectively. These hybrid samples presented a broader particle size distribution with larger particles (~200 nm in all hybrid samples), abundant large pores (100 nm), and very similar submicrostructural characteristics with an associated macroporous distribution, showing a well-branched and highly nanostructured porous network, typical of polysiloxane hydrophobic aerogels [23,33], which is in good agreement with the reported results from N_2 physisorption experiments (Table 2 and Fig. 3), making it difficult to discern the differences between them.

Liquid absorption experiments

The influence of the drying procedure and type of solvent on the absorption kinetics of the hybrid samples was evaluated by the study of the normalized weight gain, namely, the ratio $M(t)/M_\infty$ (see Fig. 7) for two different organic solvents at room temperature, hexane and silanol-terminated PDMS fluid. At first glance, Fig. 7, left, shows that the type of drying procedure does not influence the liquid absorption behaviour. Thus, the nanostructures that they exhibit are similar regarding the absorption kinetics. However, well differentiated absorption regimes for each type of solvent are observed. Due to its lower viscosity, hexane is a liquid that diffuses faster than liquid PDMS. Thus, in the case of hexane, the diffusion process happens almost instantaneously, and the saturation level M_∞ is achieved in a matter of minutes, following the normalized weight gain $M(t)/M_\infty$ vs. $t^{0.5}$ as Fick's law of diffusion fits the linear trend perfectly ($R^2 > 0.99$) before reaching saturation ($M(t)/M_\infty \approx 0.8$) [34]. In Table 3, the information about the corresponding linear curve fitting data is shown.

Non-linear absorption kinetics is observed for the liquid PDMS diffusion (Fig. 7, right), which includes swelling. In

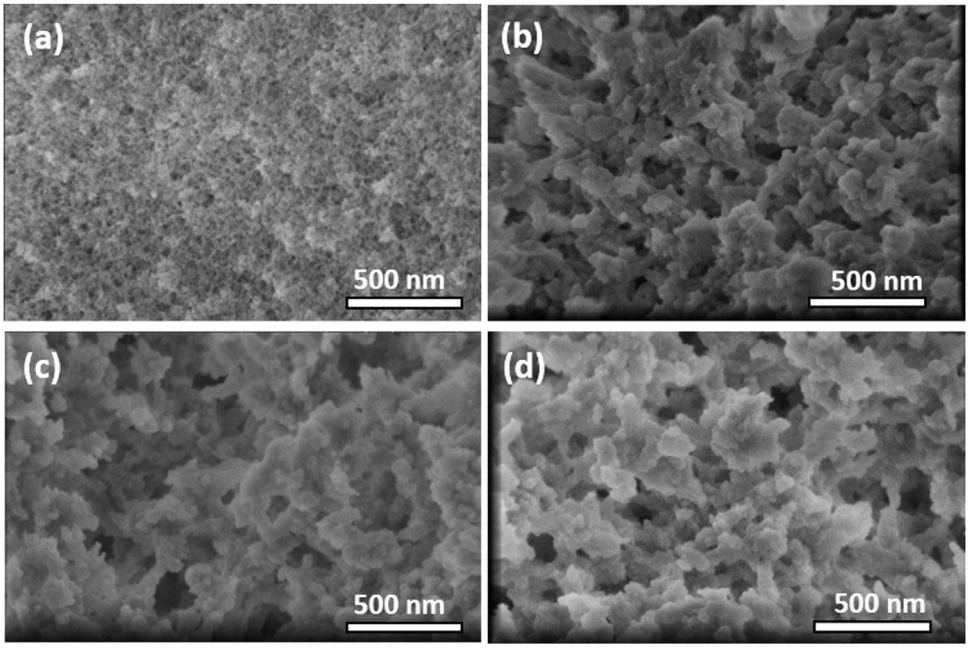

Fig. 6 – Scanning electron micrographs of (a) TD0; (b) ScEt; (c) $ScCO_2$; and (d) AD samples.

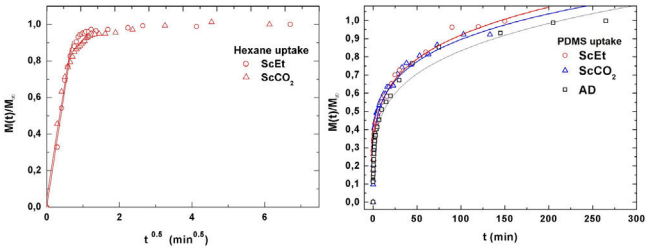

Fig. 7 – Left: normalized weight gain for hexane uptake in ScEt and $ScCO_2$ samples versus square-root of time. Lines corresponding to linear fittings performed up to ~ 80% of the process in hexane. Correlation values $R^2 > 0.99$ in all cases. Right: plots of normalize weight gain values versus time for PDMS uptake. Lines correspond to non-linear fittings according to semi-empirical power law equation for swelling of polymers [22]. Fitting parameters are shown in Table 3.

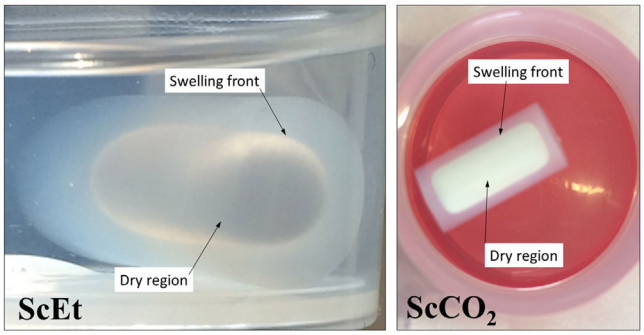

Fig. 8 – Images of the hybrid aerogels ScEt and $ScCO_2$ in an intermediate state of the absorption phenomena of liquid PDMS. The opacity of the dry samples disappears as the liquid penetrates the porous space and swells the samples.

this case, the following simple and semi-empirical power law equation is commonly used to determine the mechanism of diffusion in this type of polymeric network:

$$\frac{M(t)}{M_\infty} = kt^n \quad (2)$$

where the constants k and t, are characteristics of the solvent–polymer system and the diffusional exponent n are characteristics of the solvent–polymer system depends on the geometry of the polymeric network, as well as on the physical mechanism of the solvent uptake. The non-linear fitting curves to Eq. (2) are plotted in Fig. 7, right, for the three hybrid samples immersed in PDMS, and Table 3 summarizes the fitting parameters for each sample and solvent. The case of $n < 0.5$ refers to a slower non-fickian situation, as has resulted for the hybrid samples and liquid PDMS solvent system under study. Hence, the normalized weight gain of the absorption kinetics of liquid PDMS corresponds to non-fickian behaviour [35]. These results show that the absorption kinetics in this type of sample seems not to depend on the method of drying. On the contrary, regarding the total amount of liquid absorbed, it was observed that aerogel ScEt exhibited almost one-half of the absorption capacities of the other two hybrid samples (Table 3). Thus, while ScEt absorbed a total volume of liquid that was more than three times its own porous volume, $ScCO_2$ and AD absorbed more than six times their respective porous volumes and up to 2.6 times of the dry weight. However, the range of absorption capacities of our aerogels was lower than that of similar superhydrophobic materials prepared using methyltriethoxysilane (MTES) [36], vinyl-terminated PDMS [23] and gelatin–silica based aerogels [37], although they were in agreement with previous studies on DEDMS-based silica aerogels [5,33].

The absorption phenomenon of liquid PDMS could be directly observed thanks to the sharp well-defined boundary between the swollen and un-swollen regions of hybrid aerogels, namely, the "swelling front" indicated by the arrows in Fig. 8, therefore confirming features of non-fickian diffusion behaviour [35]. Whereas the dry hybrid samples are white and completely opaque with air inside of the pores, the uptake of the liquid PDMS reduces the opacity of the samples, allowing the clear observation of the swelling front due to the increase of the refraction index.

Mechanical properties

The porous interconnected volume, the rough surfaces observed in SEM as well as the abundant methyl content are responsible not only for the hydrophobic behaviour observed in the obtained aerogels, but also for their mechanical responses [23,36]. As a general description, the monolithic samples exhibited high compressibility and extraordinary flexibility, indicating that the hybrid networks were covalently bonded and provided high thermal and mechanical stabilities, as described below.

Table 3 – Fitting parameters of the different mathematical models considered for normalized weight gain of hexane and liquid PDMS in hybrid aerogels. Linear fittings were performed up to 80% of the process, with correlation values $R^2 > 0.99$.

	Hexane ($\rho = 0.695$ g/cm^3) Linear t $M(t)/M_\infty = a + bt^{0.5}$		PDMS ($\rho = 0.965$ g/cm^3) Non-linear t $M(t)/M_\infty = kt^n$		Absorption capacity (ratio of V_p used)
	a	b (min$^{-0.5}$)	k	n	
ScEt	−0.01 ± 0.03	1.33 ± 0.06	0.325 ± 0.004	0.233 ± 0.008	3.3
$ScCO_2$	0.03 ± 0.04	1.36 ± 0.09	0.318 ± 0.005	0.271 ± 0.009	6.5
AD	–	–	0.276 ± 0.007	0.287 ± 0.012	6.4

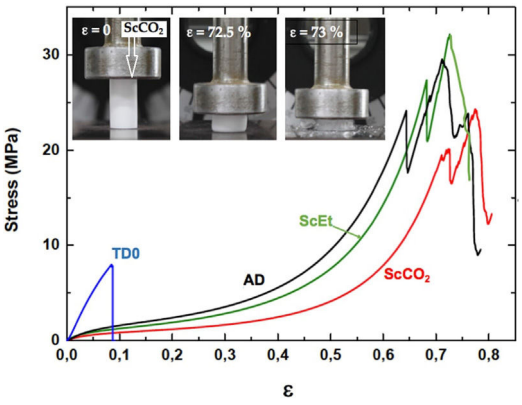

Fig. 9 – Stress–strain curves for TD0 silica aerogel and hybrid samples ScEt, $ScCO_2$ and AD, under uniaxial compression. The inset shows three different moments of the test for the sample $ScCO_2$, at the indicated strains.

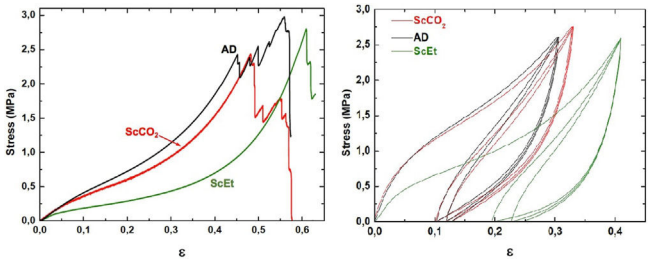

Fig. 10 – Left: stress–strain curves under uniaxial compression for hybrid samples immersed in liquid PDMS. Right: loading–unloading cyclic tests under uniaxial compression for hybrid samples immersed in liquid PDMS.

Uniaxial compression tests for as-prepared aerogels

In Fig. 9, the corresponding stress–strain curves of the TD0, ScEt, $ScCO_2$, and AD samples in the dry state are shown, providing sample-specific information about the typical mechanical behaviour, namely, the Young's modulus, compressive strength and rupture strain. All the curves of the hybrid samples exhibit a very similar initial response, much less stiff than the pure silica aerogel, followed by strain hardening up to the ultimate compressive strength, when the materials failed completely. This description corresponds to an elastomeric behaviour which is known to be rate-dependent and to exhibit hysteresis upon cyclic loading. The results are in accordance with the general behaviour previously reported for similar samples reinforced with organic contents [5,38], and in contrast to other inorganic reinforcing strategies [39]. In addition, a very slight influence of the drying method on the mechanical behaviour of the hybrid samples can be seen, and only small variations in the mechanical parameters were observed (Table 4).

TD0 showed the classical perfect elastic and brittle behaviour and fractured in a catastrophic brittle manner by rapid crack propagation with low energy release, exhibiting a relatively high Young's modulus (85.7 MPa) and low compressive strength (8.8 MPa) and rupture strain (9%) (data included in Table 4). In contrast, the compressive strength of the hybrid samples ranged from 20.5 to 27.5 MPa and Young's modulus ranged from 17.6 to 28.1 MPa, while the rupture strain varied from 64% to 72% (see Table 4). The images in the inset of Fig. 9 show the different strain stages for the $ScCO_2$ aerogel, from initial loading to the starting point of the rupture, being representative of the rest of the hybrid samples. Although similar large deformations (up to 80%) have been previously reported [36], both the compressive strength and elastic modulus of our hybrid aerogels were two to three orders of magnitude higher than those reported in most studies on this subject [33,36,40–42].

Uniaxial compression test for wet aerogels

Fig. 10 shows a series of stress–strain curves from the uniaxial compression test on the hybrid samples immersed in liquid PDMS. It was observed that these samples exhibited high swelling and associated strain softening, but retained good mechanical performance when reaching their fully swollen state. As a result, they become more compliant and the estimated corresponding mechanical parameters were significantly smaller than those of the dry samples (see Table 4). At the same time, the mechanical properties of the swollen hybrid samples allowed their handling, in contrast to the TD0 silica aerogel, which led to immediate failure at a very low strength and strain after the absorption of the liquid (data not shown). In addition, as in the dry state, no significant differences were found between the different drying procedures: similar curves and similar mechanical parameters were observed for the three hybrid samples. Nevertheless, among the set of hybrid samples, the ethanol-dried sample

Table 4 – Mechanical properties of dry and wet samples (immersed in liquid PDMS) obtained from the uniaxial compression tests.

Sample	State	Compressive strength (MPa)	Rupture strain	Young's modulus (MPa)
TD0	Dry	9 ± 4	0.10 ± 0.09	86 ± 37
	Wet	–	–	–
ScEt	Dry	28 ± 5	0.67 ± 0.05	28 ± 20
	Wet	2.8	0.61	3.2
$ScCO_2$	Dry	21 ± 2	0.72 ± 0.03	18 ± 4
	Wet	2.4	0.61	3.2
AD	Dry	24 ± 5	0.64 ± 0.02	28 ± 3
	Wet	2.4	0.45	4.45

ScEt showed the highest strain-at-break, suggesting it has the best performance in absorbing and expelling liquids, from the mechanical point of view.

To verify the usefulness of the samples for solvent recovery, cyclic loading tests were performed by uniaxial compression inside the PDMS liquid. The hybrid samples were tested in three consecutive cycles between 60% and 80% of the maximum load (Fig. 10), without any significant change in the mechanical response, except for the Mullins effect for cyclic stress, a stress-softening viscoelastic effect that takes place in rubber-like materials [43]. All the samples recovered their shapes and sizes inside the liquid bath, minutes after the last unloading. These results revealed the existence of a visco-poroelastic effect, that is, the PDMS liquid was expelled from the inner core of the cylindrical samples exhibiting a high diffusivity due to the high crosslink density of the hybrid network. This was confirmed by the good mechanical behaviour and the corresponding elastic parameters of the wet samples (see Table 4). As a result, the wet samples presented physical properties that were substantially better than other conventional absorbent gels [33,44].

Specifically, when compared to the ScEt and AD samples, the $ScCO_2$ aerogel was highly resistant to fracture and was stretchable (with elongations at break above 70%), and highly inert to chemical attack and degradation by hydrocarbon liquids such as hexane. These properties make this type of sample potentially attractive for new environmental applications as they enable selectively absorbing a wide range of organic solvents and oils from water mixtures.

Conclusions

In conclusion, monolithic, flexible, and superhydrophobic silica-DEDMS (50 wt.%) hybrid samples were synthesized by the sol–gel process assisted by sonocatalysis, followed by drying under three different conditions: two aerogels, one obtained by supercritical drying in (i) ethanol and (ii) the other by supercritical drying in CO_2, and (iii) a xerogel obtained by ambient drying. Their structure and pore size distributions were found to be dependent on the drying procedure and on the DEDMS content. It was observed that the ScEt samples were those that presented the lowest values of specific surface (80 m^2/g) and specific pore volume (0.32 m^3/g), while the $ScCO_2$ and AD samples shared very similar textural and microstructural characteristics. TGA, FTIR and water contact angle analysis confirmed that there was a different behaviour for ScEt, as it was the first to decompose thermally (270 °C) and exhibited hydrophobic behaviour ($128° \pm 2°$) instead of superhydrophobicity, as occurred with $ScCO_2$ ($153° \pm 1°$) and with the ambient dried sample ($151° \pm 5°$). From liquid absorption experiments and a characterization of their mechanical properties, it was observed that the $ScCO_2$ and AD samples displayed the best performance in terms of their structural stabilization, mechanical properties, and absorption capacity. In all cases, the diffusion of the liquid uptake follow a fickian behaviour. Consequently, they are suggested as the best option for environmental applications for oil spill and organic solvent remediation.

Acknowledgments

This work has been co-financed by the 2014–2020 ERDF Operational Programme and by the Department of Economy, Knowledge, Business and University of the Regional Government of Andalusia. Project reference: FEDERUCA18-106598. V-M.-F. thanks the grant from V Plan Propio de Investigación de la Universidad de Sevilla. Funding help for the Ayuda 2018 VI-PPTIUS and the SGI functional characterization from the CITIUS-Central services of the University of Seville are also acknowledged. Mr. Adrián Pavón Duarte is deeply acknowledged for his help during simple drying.

REFERENCES

[1] J.S.A. Cortez, B.I. Kharisov, T.E.S. Quezada, T.C.H. García, Micro- and nanoporous materials capable of absorbing solvents and oils reversibly: the state of the art, Pet. Sci. 14 (2017) 84–104, http://dx.doi.org/10.1007/s12182-016-0143-0.
[2] B. Ge, X. Men, X. Zhu, Z. Zhang, A superhydrophobic monolithic material with tunable wettability for oil and water separation, J. Mater. Sci. 50 (2015) 2365–2369, http://dx.doi.org/10.1007/s10853-014-8756-4.
[3] G. Ozan Aydin, H. Bulbul Sonmez, Organic–inorganic hybrid gels for the selective absorption of oils from water, Environ. Sci. Pollut. Res. 23 (2016) 11695–11707, http://dx.doi.org/10.1007/s11356-016-6342-9.
[4] D. Wang, E. Mclaughlin, R. Pfeffer, Y.S. Lin, Adsorption of oils from pure liquid and oil–water emulsion on hydrophobic silica aerogels, Sep. Purif. Technol. 99 (2012) 28–35, http://dx.doi.org/10.1016/j.seppur.2012.08.001.
[5] V. Morales-Florez, M. Piñero, V. Braza, M. del Mar Mesa, L. Esquivias, N. de la Rosa-Fox, Absorption capacity, kinetics and mechanical behaviour in dry and wet states of hydrophobic DEDMS/TEOS-based silica aerogels, J. Sol–Gel Sci. Technol. 81 (2017) 600–610, http://dx.doi.org/10.1007/s10971-016-4203-0.
[6] J.G. Reynolds, P.R. Coronado, L.W. Hrubesh, Hydrophobic aerogels for oil-spill cleanup – intrinsic absorbing properties, Energy Sources 23 (2001) 831–843, http://dx.doi.org/10.1080/009083101316931906.
[7] V. Morales-Flórez, M. Piñero, N. de la Rosa-Fox, L. Esquivias, J.A. Anta, J. Primera, The cluster model: a hierarchically-ordered assemblage of random-packing spheres for modelling microstructure of porous materials, J. Non. Cryst. Solids 354 (2008), http://dx.doi.org/10.1016/j.jnoncrysol.2007.07.061.
[8] J. Phalippou, T. Woignier, R. Rogier, Fracture toughness of silica aerogels, J. Physyique Colloq. 50 (1989) 191–196, http://dx.doi.org/10.1051/jphyscol:1989431.
[9] A. Venkateswara Rao, D. Haranath, Effect of methyltrimethoxysilane as a synthesis component on the hydrophobicity and some physical properties of silica aerogels, Micropor. Mesopor. Mater. 30 (1999) 267–273, http://dx.doi.org/10.1016/S1387-1811(99)00037-2.
[10] S. Kramer, F. Rubio-Alonso, J.D. Mackenzie, Organically modified silicate aerogels, Aeromosils 435 (1996) 295–300, http://dx.doi.org/10.1557/PROC-435-295.
[11] N. de la Rosa-Fox, V. Morales-Flórez, J.A. Toledo-Fernández, M. Piñero, R. Mendoza-Serna, L. Esquivias, Nanoindentation on hybrid organic/inorganic silica aerogels, J. Eur. Ceram. Soc. 27 (2007) 3311–3316, http://dx.doi.org/10.1016/j.jeurceramsoc.2007.02.209.

[12] V. Morales-Flórez, J.A. Toledo-Fernández, N. De La Rosa-Fox, M. Piñero, L. Esquivias, Percolation of the organic phase in hybrid organic–inorganic aerogels, J. Sol–Gel Sci. Technol. 50 (2009), http://dx.doi.org/10.1007/s10971-008-1874-1.
[13] K. Morita, Y. Hu, J.D. Mackenzie, The effect of ultrasonic radiation on gelation and properties of ormosils, Mater. Res. Soc. Symp. Proc. 271 (1992) 693–698.
[14] L. Esquivias, N. Pinero, M. Morales-Florez, V. Rosa-Fox, Aerogels synthesis by sonocatalysis: sonogels, in: M.M. Koebel, M.A. Aegerter, N. Leventis (Eds.), Aerogels Handbook, 1st ed., Springer Link, New York, NY, USA, 2011, pp. 419–445, http://dx.doi.org/10.1007/978-1-4419-7589-8.
[15] H. Maleki, L. Durães, A. Portugal, An overview on silica aerogels synthesis and different mechanical reinforcing strategies, J. Non. Cryst. Solids 385 (2014) 55–74, http://dx.doi.org/10.1016/j.jnoncrysol.2013.10.017.
[16] N. De La Rosa-Fox, V. Morales-Flórez, J.A. Toledo-Fernández, M. Piñero, L. Esquivias, U. Keiderling, SANS study of hybrid silica aerogels under "in situ" uniaxial compression, J. Sol–Gel Sci. Technol. 45 (2008), http://dx.doi.org/10.1007/s10971-008-1686-3.
[17] L.T. Zhuravlev, The surface chemistry of amorphous silica. Zhuravlev model, Colloids Surf. A: Physicochem. Eng. Asp. 173 (2000) 1–38, http://dx.doi.org/10.1016/S0927-7757(00)00556-2.
[18] A.M. Anderson, M.K. Carroll, E.C. Green, J.T. Melville, M.S. Bono, Hydrophobic silica aerogels prepared via rapid supercritical extraction, J. Sol–Gel Sci. Technol. 53 (2010) 199–207, http://dx.doi.org/10.1007/s10971-009-2078-z.
[19] A.V. Rao, M.M. Kulkarni, D.P. Amalnerkar, T. Seth, Superhydrophobic silica aerogels based on methyltrimethoxysilane precursor, J. Non. Cryst. Solids 330 (2003) 187–195, http://dx.doi.org/10.1016/j.jnoncrysol.2003.08.048.
[20] N. De la Rosa-Fox, M. Piñero, L. Esquivias, Organic–inorganic hybrid materials form sonogels, in: H.S. Nalwa (Ed.), Handb. Org. Hybrid Mater. Nanocomposites, American Scientific Publishers, 2003.
[21] M. Aegerter, N. Leventis, M. Koebel, Aerogels Handbook (Advances in Sol–Gel Derived Materials and Technologies), Springer-Verlag New York Inc, 2011.
[22] H. Zhang, F. Yang, R. Bai, Z. Zhao, J. Li, X. Zeng, X. Zhang, APD compressible aerogel-like monoliths with potential use in environmental remediation, Materials (Basel) 12 (2019) 1–10, http://dx.doi.org/10.3390/ma12203459.
[23] F. Zou, L. Peng, W. Fu, J. Zhang, Z. Li, Flexible superhydrophobic polysiloxane aerogels for oil-water separation via one-pot synthesis in supercritical CO_2, RSC Adv. 5 (2015) 76346–76351, http://dx.doi.org/10.1039/c5ra13023a.
[24] E.J. Park, Y.K. Cho, D.H. Kim, M.G. Jeong, Y.H. Kim, Y.D. Kim, Hydrophobic polydimethylsiloxane (PDMS) coating of mesoporous silica and its use as a preconcentrating agent of gas analytes, Langmuir 30 (2014) 10256–10262, http://dx.doi.org/10.1021/la502915.
[25] A. Venkateswara Rao, N.D. Hegde, H. Hirashima, Absorption and desorption of organic liquids in elastic superhydrophobic silica aerogels, J. Colloid Interface Sci. 305 (2007) 124–132, http://dx.doi.org/10.1016/j.jcis.2006.09.025.
[26] L. Qi, X. Tang, Z. Wang, X. Peng, Pore characterization of different types of coal from coal and gas outburst disaster sites using low temperature nitrogen adsorption approach, Int. J. Min. Sci. Technol. 27 (2017) 371–377, http://dx.doi.org/10.1016/j.ijmst.2017.01.005.
[27] W.C. Wu, C.C. Chuang, J.L. Lin, Bonding geometry and reactivity of methoxy and ethoxy groups adsorbed on powdered TiO_2, J. Phys. Chem. B 104 (2000) 8719–8724, http://dx.doi.org/10.1021/jp0017184.
[28] M.S. Kavale, D.B. Mahadik, V.G. Parale, A.V. Rao, P.B. Wagh, S.C. Gupta, Methyltrimethoxysilane based flexible silica aerogels for oil absorption applications, AIP Conf. Proc. 1447 (2012) 1283–1284, http://dx.doi.org/10.1063/1.4710481.
[29] R. Al-Oweini, H. El-Rassy, Synthesis and characterization by FTIR spectroscopy of silica aerogels prepared using several Si(OR)4 and $R''Si(OR')_3$ precursors, J. Mol. Struct. 919 (2009) 140–145, http://dx.doi.org/10.1016/j.molstruc.2008.08.025.
[30] M.L.N. Perdigoto, R.C. Martins, N. Rocha, M.J. Quina, L. Gando-Ferreira, R. Patrício, L. Durães, Application of hydrophobic silica based aerogels and xerogels for removal of toxic organic compounds from aqueous solutions, J. Colloid Interface Sci. 380 (2012) 134–140, http://dx.doi.org/10.1016/j.jcis.2012.04.062.
[31] M. Łączka, K. Cholewa-Kowalska, M. Kogut, Organic–inorganic hybrid glasses of selective optical transmission, J. Non. Cryst. Solids 287 (2001) 10–14, http://dx.doi.org/10.1016/S0022-3093(01)00532-4.
[32] H.J. Kleebe, H. Störmer, S. Trassl, G. Ziegler, Synthesis of polymeric precursors for the formation of nanocrystalline Ti–C–N/amorphous Si–C–N composites, Appl. Organomet. Chem. 15 (2001) 879–886, http://dx.doi.org/10.1002/aoc.241.
[33] Y. Zhang, Q. Shen, X. Li, H. Xie, C. Nie, Facile synthesis of ternary flexible silica aerogels with coarsened skeleton for oil–water separation, RSC Adv. 10 (2020) 42297–42304, http://dx.doi.org/10.1039/d0ra07906e.
[34] J. Gierszewska-Drużyńska, Magdalena Ostrowska-Czubenko, Mechanism of water diffusion into noncrosslinked and ionically crosslinked chitosan membranes, Prog. Chem. Appl. Chitin ItsMec Deriv. 17 (2012) 59–66.
[35] M.L. Bruschi, Mathematical Models of Drug Release, Elsevier, 2015, http://dx.doi.org/10.1016/b978-0-08-100092-2.00005-9.
[36] Y. Yu, X. Wu, D. Guo, J. Fang, Preparation of flexible, hydrophobic, and oleophilic silica aerogels based on a methyltriethoxysilane precursor, J. Mater. Sci. 49 (2014) 7715–7722, http://dx.doi.org/10.1007/s10853-014-8480-0.
[37] L. Yun, J. Zhao, X. Kang, Y. Du, X. Yuan, X. Hou, Preparation and properties of monolithic and hydrophobic gelatin–silica composite aerogels for oil absorption, J. Sol–Gel Sci. Technol. 83 (2017) 197–206, http://dx.doi.org/10.1007/s10971-017-4378-z.
[38] M. Pinñero, V. Morales-Flórez, N. de La Rosa-Fox, L. Esquivias, Mechanical properties of silica hybrid aerogels|Propiedades mecánicas de aerogeles híbridos de sílice, Bol. La Soc. Esp. Ceram. y Vidr. 44 (2005) 291–293.
[39] M. Piñero, M.M. Mesa-Díaz, D. de los Santos, M.V. Reyes-Peces, J.A. Díaz-Fraile, N. de la Rosa-Fox, L. Esquivias, V. Morales-Florez, Reinforced silica-carbon nanotube monolithic aerogels synthesised by rapid controlled gelation, J. Sol–Gel Sci. Technol. 86 (2018) 391–399, http://dx.doi.org/10.1007/s10971-018-4645-7.
[40] J. He, H. Zhao, X. Li, D. Su, F. Zhang, H. Ji, R. Liu, Superelastic and superhydrophobic bacterial cellulose/silica aerogels with hierarchical cellular structure for oil absorption and recovery, J. Hazard. Mater. 346 (2018) 199–207, http://dx.doi.org/10.1016/j.jhazmat.2017.12.045.
[41] M. Li, H. Jiang, D. Xu, Preparation of sponge-reinforced silica aerogels from tetraethoxysilane and methyltrimethoxysilane for oil/water separation, Mater. Res. Express. 5 (2018) 1–10, http://dx.doi.org/10.1088/2053-1591/aab7c3.

[42] L. Li, T. Hu, Y. Yang, J. Zhang, Strong, compressible, bendable and stretchable silicone sponges by solvent-controlled hydrolysis and polycondensation of silanes, J. Colloid Interface Sci. 540 (2019) 554–562, http://dx.doi.org/10.1016/j.jcis.2019.01.059.
[43] C.M. Roland, The Mullins effect in crosslinked rubber, J. Rheol. 33 (1989) 659–670, http://dx.doi.org/10.1122/1.550032.
[44] I. Benito-González, A. López-Rubio, L.G. Gómez-Mascaraque, M. Martínez-Sanz, PLA coating improves the performance of renewable adsorbent pads based on cellulosic aerogels from aquatic waste biomass, Chem. Eng. J. 390 (2020) 124607, http://dx.doi.org/10.1016/j.cej.2020.124607.